



**Universiteit
Leiden**
The Netherlands

Water on well-defined platinum surfaces : an ultra high vacuum and electrochemical study

Niet, M.J.T.C. van der

Citation

Niet, M. J. T. C. van der. (2010, October 14). *Water on well-defined platinum surfaces : an ultra high vacuum and electrochemical study*. Retrieved from <https://hdl.handle.net/1887/16035>

Version: Corrected Publisher's Version

License: [Licence agreement concerning inclusion of doctoral thesis in the Institutional Repository of the University of Leiden](#)

Downloaded from: <https://hdl.handle.net/1887/16035>

Note: To cite this publication please use the final published version (if applicable).

Ἄριστον μὲν ὕδωρ

Πίνδαρος, Ολυμπόνικοι 1.1
(522–438 BC)

8

Hydrophobic interactions between amorphous solid water and pre-adsorbed D on the stepped Pt(533) surface

Abstract *We have studied the interaction of Pt(533) with varying coverages of water and varying coverages of pre-adsorbed deuterium under ultra high vacuum conditions. We use temperature programmed desorption and reflection absorption infrared spectroscopy techniques to study the properties of these layers. Results show that deuterium's preference to adsorb at step edges nulls the step-induced stabilization of water through an electronic effect. However, deuterium atoms at step edges do not block adsorption sites for water and water still wets the entire (111) terrace. With increasing deuterium coverage on terraces, formation of smaller, less ordered water structures replaces formation of hexamer ring structures. Near deuterium saturation, water preferentially forms 3-dimensional amorphous solid water (ASW) clusters at the steps. The typical phase transition of ASW to crystalline ice is observed in these clusters. Although exchange of D_{ad} with H_2O occurs both at steps and terraces and is dependent on both surface coverages, the preference of water molecules to cluster at the step sites on the hydrophobic, deuterium-saturated Pt(533) surface biases exchange toward steps.*

8.1 Introduction

The interaction between water and platinum surfaces has been studied extensively, because of its importance in electrochemistry, fuel cell catalysis, heterogeneous catalysis, and corrosion chemistry. Three extensive reviews have appeared that summarize the large body of knowledge on water-surface interactions that has been obtained using a variety of surfaces, co-adsorbates, and employed techniques.⁶⁻⁸

Most studies investigating the platinum-water interaction have used the (111) surface as a model. Although this is the least complex system, ultra high vacuum (UHV) studies already show significant complexity in adsorption and desorption phenomena.¹¹⁸⁻¹²⁰ However, a real catalytic surface contains additional low coordination or defect sites. These defect sites are often thought to be more active for catalytic reactions involving bond breaking and making. Although some experiments have focused on the influence of steps and defects that are naturally present on a Pt(111) crystal,^{28,29} more insight results from studies employing a better-defined model, such as a regularly stepped surface.^{26,27} Co-adsorption of water with hydrogen, which is of particular interest to understanding the chemistry occurring at the anode of low temperature fuel cells and the reversible hydrogen electrode (RHE), has received even less attention so far.^{6,7}

The general consensus is that on Pt(111) water adsorbs molecularly at all coverages and temperatures (< 180 K). Classically, water adsorbed on metal surfaces is thought to form an ice-like bilayer of hexagonal rings.⁶⁻⁸ A combined scanning tunneling microscopy (STM) and density functional theory (DFT) study finds that at submonolayer coverages water islands also contain pentagon and heptagon ring structures.¹⁹ Water dosed on Pt(111) at temperatures well below 135 K yields growth of amorphous solid water (ASW).²¹ Temperature programmed desorption (TPD) studies of ASW show two peaks. One peak at 171 K is associated with monolayer desorption. This peak shows the characteristics of zero-order desorption kinetics²² and has been attributed to co-existence of a condensed phase and a 2-dimensional water-gas at sub-monolayer coverages.²¹ A second peak, associated with desorption from multilayers, starts at 154 K and increases in temperature with coverage.²³ Multilayers have been shown to crystallize during the TPD-ramp.^{21,147} On stepped surfaces water adsorbs preferentially on step sites, forming molecular chains.²⁸ TPD shows a stabilization of the water monolayer by the presence of step sites.^{26,27} A two peak structure is observed for a monolayer of H₂O desorbing from the stepped Pt(533) surface (Pt[4(111) × (100)]). The high temperature peak is associated with desorption from step sites, whereas the low temperature peak is associated with desorption from terrace sites.²⁷

Molecular hydrogen adsorbs dissociatively on both Pt(111)⁵⁵⁻⁵⁷ and stepped platinum surfaces.^{55,58,60-64} TPD experiments of hydrogen desorbing from Pt(533) show two desorption features: a large feature below 360 K and a smaller feature

at 380 K.⁶³ The high temperature feature is associated with recombinative desorption from step sites, whereas the lower temperature desorption feature is associated with recombinative desorption from terrace sites and possibly some remaining step sites. This indicates preferential adsorption of hydrogen on step sites.

We have described the adsorption of both water and deuterium on the stepped Pt(533) surface in detail in chapter 3.

The co-adsorption of water and hydrogen is especially relevant for electrochemistry. Water desorbing from a hydrogen covered Pt(111) surface develops a new peak at higher desorption temperatures at the expense of the water desorption feature at 170 K. The desorption temperature of this feature goes through a maximum at 176 K as a function of D₂ pre-dose. However, at all deuterium pre-coverages the new feature appears at higher temperatures than for the bare surface.⁹⁰ Interestingly, on Pt(100) the desorption temperature decreases on the hydrogen covered surface compared to the bare surface.⁹¹

There is no experimental data on the co-adsorption of H₂O and H_{ad} on a stepped surface. However, as noted earlier, in order to understand what is happening on a real catalyst it is vital to know the influence of step and defect sites on the structure and stability of water and the catalytic activity. Therefore, we use TPD and RAIRS in conjunction with isotope labeling to investigate the influence of pre-adsorbed hydrogen (deuterium) on co-adsorbed H₂O on the stepped Pt(533) surface in UHV.

8.2 Experimental

Experiments were performed in POTVIS. General procedures are given in chapter 2.1.5.

The QMS signals for H₂, HD, and D₂ were calibrated using full monolayer TPD spectra. Step and terrace peaks were treated separately by fitting two Gaussian functions to the data. Since it is not possible to obtain a full HD layer, the HD signal was calibrated dosing approximately equal amounts of H₂ and D₂ simultaneously at a total pressure of 2×10^{-7} mbar. The measured hydrogen (deuterium) fraction, $\phi_{\text{H}_2,\text{eq}}$ ($\phi_{\text{D}_2,\text{eq}}$), can be obtained by comparing the H₂ (D₂) signal to the one of a full monolayer. Assuming that H_{ad} and D_{ad} are at equilibrium at the surface and that there is no isotope effect for recombination of the atoms, the other fractions are given by:

$$\phi_{\text{D}_2,\text{eq}} = \left(1 - \sqrt{\phi_{\text{H}_2,\text{eq}}}\right)^2 \quad (8.1)$$

$$\phi_{\text{HD},\text{eq}} = 2 - 2\sqrt{\phi_{\text{H}_2,\text{eq}}} - 2\left(1 - \sqrt{\phi_{\text{H}_2,\text{eq}}}\right)^2 \quad (8.2)$$

RAIRS spectra were taken at a resolution of 4 cm^{-1} using a Fourier transform infrared (FTIR) spectrometer (Biorad FTS 175). A series of flat and parabolic gold

coated mirrors focuses the light onto the sample and finally onto an external liquid nitrogen cooled mercury cadmium telluride (MCT) detector. A KRS-5 wire grid polarizer is mounted on the window where the beam enters the UHV chamber to enhance the signal to noise ratio. The sample temperature during scans was 100 K.

8.3 Results

Figure 8.1 shows TPD spectra of D₂ ($m/e = 4$) desorbing from Pt(533). For all spectra, we dosed D₂ in excess of the required amount for saturating the surface from background dosing.⁶³ We start dosing at $T_{\text{crystal}} = 500$ K and cool the crystal consecutively to below 120 K. This procedure minimizes simultaneous H₂ adsorption from UHV residual gas. Trace 8.1c shows two peaks generally observed in hydrogen desorption from stepped platinum surfaces.⁶⁶ The peaks at ~ 370 K and ~ 260 K are generally ascribed to associative desorption from (100) steps and (111) terraces, respectively.^{63,66} Although a saturation value of 0.9 ± 0.05 ML has been reported,⁶³ we can not confirm this value here. We simply refer to the saturated surface by $\theta_{\text{D}} = 1$, without implying a $D_{\text{ad}} : \text{Pt}$ ratio of 1 : 1. The ratio of terrace versus step desorption, as determined from Gaussian fits to the individual peaks at $\theta_{\text{D}} = 1$, yields 3 : 1. This value is strongly dependent on acceptance angle of the differentially pumped QMS, as we will discuss in a separate publication.⁷⁴ Trace 8.1a shows desorption of D₂ after annealing the deuterium-saturated surface for 180 s at 280 K, followed by quenching to < 100 K. This extra annealing step removes nearly all deuterium required to saturate the terraces while desorption from steps remains unaltered. Trace 8.1b shows that annealing at lower temperatures allows

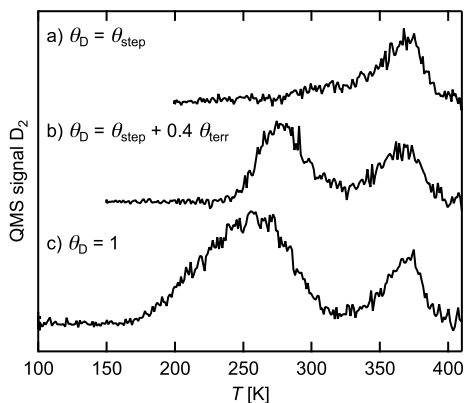


Figure 8.1 TPD of D₂ after saturation dose on Pt(533) (adsorbed while cooling down from 500 to 120 K) without annealing a), 180 s annealing at 240 K b), and 180 s annealing at 280 K c).

for controlling the amount of removed deuterium from the (111) terraces. We have found that this procedure yields reproducible surface coverages of deuterium and minimizes contamination by simultaneous co-adsorption of H_2 from residual gas.

Figure 8.2 shows TPD spectra for $m/e = 18$ and 19 after dosing various amounts of H_2O onto Pt(533) containing different deuterium pre-coverages. For clarity, we do not show the TPD spectra for $m/e = 20$, since they show the same characteristics compared to $m/e = 19$, but are much less intense. We have verified that cracking in the QMS ionizer of HOD and D_2O yields no significant contribution to the signal at $m/e = 18$ at the low signal intensities in experiments for $m/e = 19$ and 20. Therefore, the signal at $m/e = 18$ results from H_2O only within our experimental error. Similarly, the signal at $m/e = 19$ results only from HOD and the signal at $m/e = 20$ only results from D_2O . In figure 8.2c, water desorbs from bare Pt(533), *i.e.* $\theta_{\text{D}} = 0$. In figure 8.2b, we have removed deuterium using the pre-annealing step to the extent that θ_{D} equals the amount required to saturate the steps, *i.e.* $\theta_{\text{D}} \approx \theta_{\text{step}}$. In figure 8.2a, H_2O is dosed directly after dosing a saturation coverage of deuterium, *i.e.* $\theta_{\text{D}} = 1$.

Detailed inspection of the TPD spectra in figure 8.2 yields the following observations. We focus first on the traces for H_2O (plotted versus the left axis). Three peaks, $\alpha_1 - \alpha_3$, with peak temperatures of, respectively, ~ 188 K, ~ 171 K, and ~ 148 K are observed. The α_1 peak appears at the lowest H_2O coverages. The second peak, α_2 , is clearly observed prior to saturation of the first peak. The α_3 peak is only observed when the other two peaks have saturated. Following Grecea *et al.*,²⁷ we use the largest combined integral for the two high temperature peaks as a reference for the amount of adsorbed H_2O and refer to this amount as $\theta_{\text{H}_2\text{O}} = 1$ ML. Dosing larger quantities leads to the appearance of the α_3 peak, which has previously been shown to result from multilayer desorption.²⁷ When pre-adsorbing deuterium at $\theta_{\text{D}} \approx \theta_{\text{step}}$, TPD spectra for post-dosed H_2O only show two peaks, β_1 and β_2 . Their peak maxima occur at 171 K and 148 K for the highest H_2O coverage shown here. The β_1 peak saturates prior to the appearance of the β_2 peak. The peak desorption temperature of β_1 shifts from 164 K to 171 K with increasing dose. When pre-adsorbing deuterium at $\theta_{\text{D}} = 1$, TPD spectra show a single peak, γ_1 , initially appearing near 150 K. Desorption characteristics for this peak are typical for zero-order desorption kinetics, *i.e.* overlapping leading edges and a peak desorption temperature that increases with dose. Interestingly, all TPD traces for $\theta_{\text{H}_2\text{O}} \geq 0.42$ ML and $\theta_{\text{D}} = 1$ show a splitting of the peak near the maximum desorption rate. We observe this behavior already at $\theta_{\text{H}_2\text{O}} = 0.26$ ML (not shown here).

Next, we turn to the HOD signals in figure 8.2 (plotted vs right axis). Here, we first note that we are not aware of an unambiguous means to determine the integral for 1 ML HOD desorbing from the surface. Therefore, we have used the integral for 1 ML H_2O as our reference in calculating θ_{HOD} . We feel this is justified since the ionization efficiency in our QMS, the transmission through the quadrupole, and

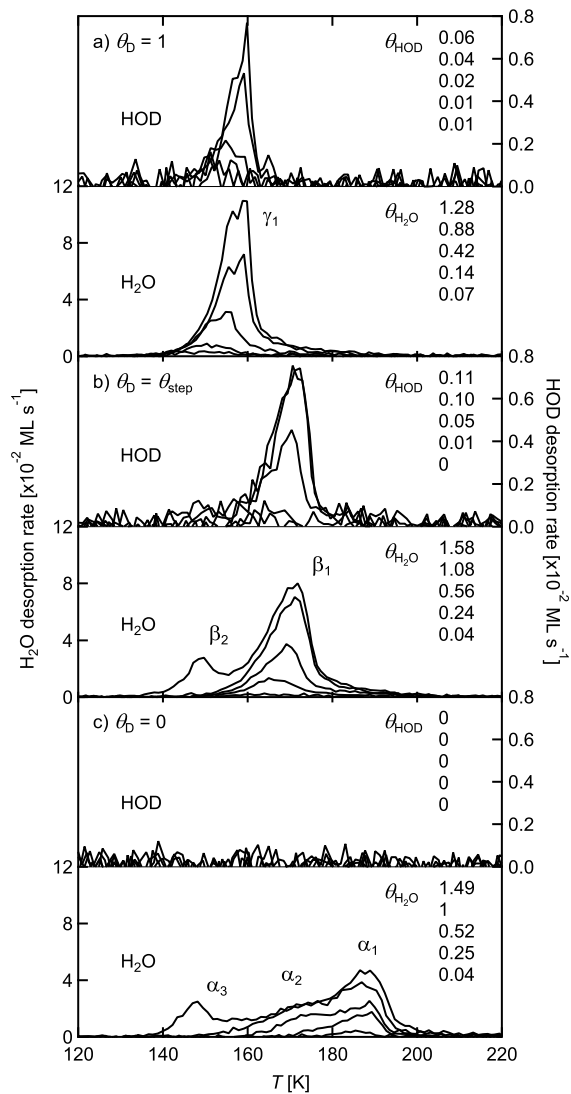


Figure 8.2 TPD spectra of H₂O (left axis) and HOD (right axis) dosed on Pt(533) with a) $\theta_D = 1$, b) $\theta_D = \theta_{step}$, and c) $\theta_D = 0$.

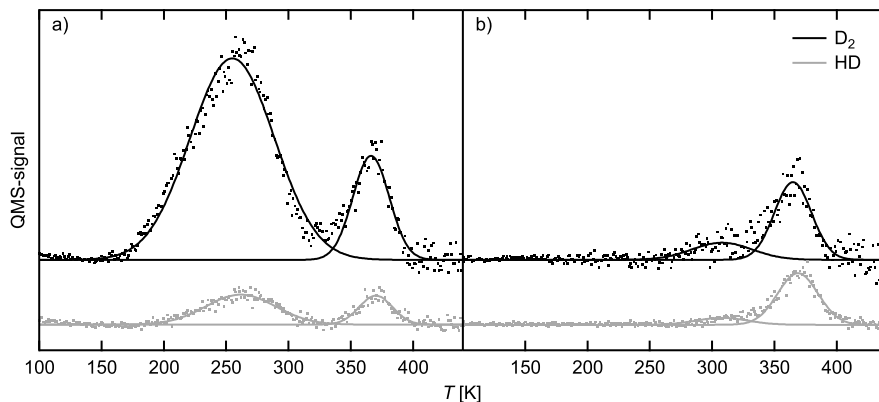


Figure 8.3 TPD spectra of $m/e = 3$ (gray) and 4 (black) for a) $\theta_D = 1$ and $\theta_{\text{H}_2\text{O}} = 0.94$ and b) $\theta_D \approx \theta_{\text{step}}$ and $\theta_{\text{H}_2\text{O}} = 0.46$ dosed on Pt(533). The solid lines show fits of two Gaussian functions to the data.

the amplification by the channeltron are not expected to vary significantly for these isotopes. Turning to the data, we observe that adsorbing H_2O on bare Pt(533) leads to no measurable desorption of HOD for any dose shown here. In contrast, HOD desorption does occur from the deuterium pre-covered surfaces in figures 8.2a and b. At $\theta_D \approx \theta_{\text{step}}$, HOD desorbs simultaneous with β_1 . For the largest water post-dose we also observe a small amount of HOD desorbing simultaneous with β_2 . For $\theta_D = 1$, HOD also desorbs simultaneous with H_2O in the peak labeled γ_1 . Here, we also observe overlapping leading edges and a change in desorption rate in the rising part of the traces.

We have integrated all TPD spectra for the three isotopes of water (H_2O , HOD, and D_2O) for varying deuterium pre-coverages. A plot of the sum of the integrated areas for these isotopes versus dose time indicates that the total quantity of desorbing water varies linearly with dose time. The slope of such a plot is a measure of the sticking probability. We observe that the sticking probability does not change significantly by pre-dosing any amount of deuterium, although minor changes appear comparable to our estimated experimental error. The absolute sticking probability for H_2O on Pt(533) was determined by Grecea *et al.*, and found to be 1.27 .

Figure 8.3 shows TPD spectra of $m/e = 3$ (HD) and $m/e = 4$ (D_2) for different $\theta_D / \theta_{\text{H}_2\text{O}}$ coverages. The signal at $m/e = 2$ (H_2) was not usable for analysis, because of the large background signal caused by objects other than the sample warming up and degassing H_2 during heating. Trace 8.3a was obtained after fully saturating the surface with D_{ad} , prior to adsorbing 0.94 ML H_2O . Two features are seen in both the HD and the D_2 signal: a high temperature feature at 365 K and a low temperature feature at 255 K. The high temperature feature is associated with

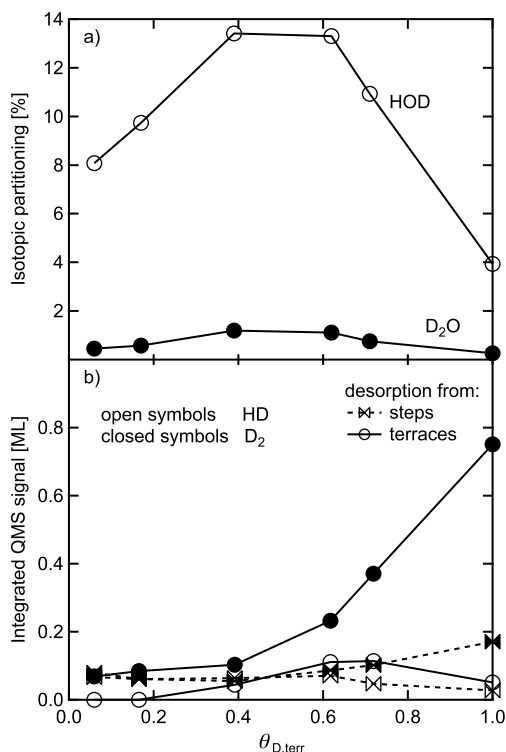


Figure 8.4 a) Isotopic partitioning in water TPD spectra for a range of deuterium coverages on the (111) terraces of Pt(533). b) Absolute amounts of subsequently desorbing HD and D₂, separated into step and terrace contributions.

desorption from step sites, whereas the low temperature feature is associated with desorption from terrace sites.⁶³ It can be clearly seen that the ratio $HD_{step} : D_{2,step}$ is much larger than the ratio $HD_{terrace} : D_{2,terrace}$. This shows that, at least relatively, HD is formed more on step sites than on terrace sites. Trace 8.3b show HD and D₂ desorption traces when step sites are fully covered with D_{ad} and $\theta_{H_2O} = 0.46$ ML. Both the HD and D₂ signals show desorption from step sites only.

Figure 8.4a plots the fraction of HOD and D₂O appearing in water TPD spectra for varying deuterium pre-coverages on the (111) terraces. Note that in our experiments, we must use deuterium-coverages of $\theta_D \geq \theta_{step}$, since leaving part of the steps bare results in contamination from residual H₂ in the UHV system. For both HOD and D₂O, we observe in figure 8.4a that their appearance is strongly dependent on the fractional deuterium pre-coverage of the (111) terraces. Production of the deuterated species peaks when terraces are approximately half covered with deuterium. Figure 8.4b shows the absolute amounts of HD and D₂ desorb-

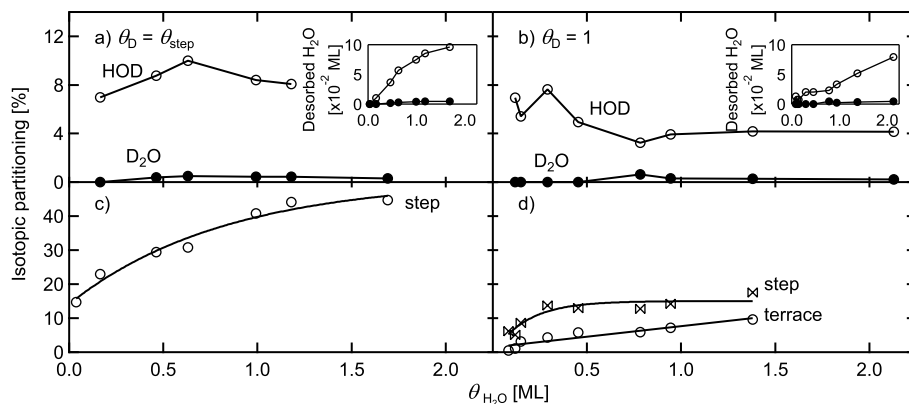


Figure 8.5 Isotopic partitioning for varying water coverages on Pt(533) with a) and c) $\theta_{\text{D}} \approx \theta_{\text{step}}$ and b) and d) $\theta_{\text{D}} = 1$. A) and b) show the HOD (D_2O) fractions (insets show absolute amounts), whereas c) and d) show the HD fractions, deconvoluted into terrace and step contributions. The lines are only a guide for the eye.

ing from the surface. Step (squares and dashed line) and terrace (circles and solid line) contributions are indicated separately. We observe a maximum in the amount of HD adsorbing from terrace sites at $\theta_{\text{D, terr}} \approx 0.65$ whereas the amount of D_2 desorbing from terrace sites increases continuously with increasing $\theta_{\text{D, terr}}$. The amounts of HD and D_2 desorbing from step sites only vary significantly when θ_{D} is close to unity. The total water desorption varied slightly in these experiments ($0.94 < \theta_{\text{H}_2\text{O}} < 1.3$ ML). We have normalized the results in figure 8.4 for this slight variation.

Figure 8.5a shows the dependence of the isotopic partitioning in water for varying amounts of water dosed after creating a deuterium coverage of $\theta_{\text{D}} \approx \theta_{\text{step}}$. Figure 8.5b shows same dependence for $\theta_{\text{D}} = 1$. The insets show the absolute signals. For the step-covered deuterium surface we observe maximum partitioning of deuterated isotopes for $\theta_{\text{H}_2\text{O}} \sim 0.6$, although the dependence on water coverage is less pronounced than the dependence on the deuterium coverage (figure 8.4). For $\theta_{\text{H}_2\text{O}} \geq 1.2$ ML, the absolute HOD signal starts to level off. For the saturated deuterium surface, the relative yield of deuterated water is slightly higher for $\theta_{\text{H}_2\text{O}} < 1$ ML than for $\theta_{\text{H}_2\text{O}} > 1$ ML. The absolute amount of desorbing HOD increases linearly with $\theta_{\text{H}_2\text{O}}$. Figures 8.5c and 8.5d show the isotopic partitioning of desorbing HD. Here, we are able to determine the partitioning without use of the H_2 signal, since we have determined the absolute value of maximum integral for HD desorbing from step and terrace sites (see section 8.2). For $\theta_{\text{D}} \approx \theta_{\text{step}}$ the fraction of desorbing HD initially increases linearly. When $\theta_{\text{H}_2\text{O}}$ becomes larger than ~ 1.2 ML the fraction of desorbing HD starts to level off. On the D-saturated sur-

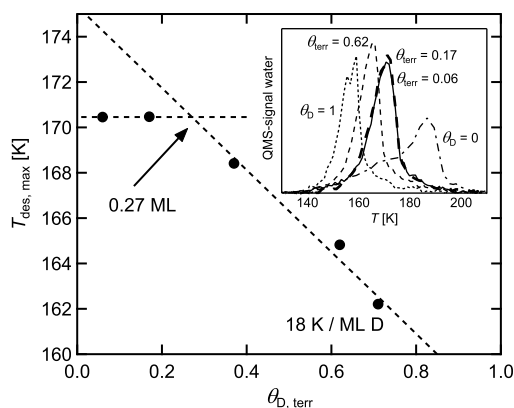


Figure 8.6 Temperature of maximum desorption rate for varying deuterium pre-coverages of the Pt(533) (111) terraces when ~ 1 ML water is adsorbed. The inset shows the corresponding original TPD spectra.

face the fraction of HD formed on terrace sites keeps increasing linearly with H₂O dose. On step sites it levels off at $\theta_{\text{H}_2\text{O}} > 0.3$ ML. The fractional isotopic exchange is consistently larger at step sites than at terrace sites.

The inset of figure 8.6 shows TPD spectra for water with varying deuterium pre-coverages. Here, the TPD signals are the summed signals for $m/e = 18, 19$ and 20 . The total water coverage varies only slightly between 0.94 and 1.3 ML, whereas the deuterium pre-coverage ranges from 0 to 1 . Noteworthy is the complete disappearance of the α_1 peak at 188 K upon pre-adsorption of deuterium at the coverage required to saturate the steps. For $\theta_{\text{D}} > \theta_{\text{step}}$, we observe that the temperature of the desorption peak maximum lowers. In figure 8.6, we show the temperature of maximum desorption rate as a function of terrace occupancy. Also, we note that in the inset of figure 8.6, the splitting of the desorption feature appears only at the highest deuterium pre-coverage. We start observing this behavior from $\theta_{\text{D, terr}} > 0.70$ onward (not shown here).

The upper line in figure 8.7a shows the RAIRS spectrum of 1 ML H₂O adsorbed on the bare Pt(533) surface. The spectrum shows two features at 3384 and at 3684 cm^{-1} . The feature at 3384 cm^{-1} is associated with the OH stretching (ν_{OH}) mode of hydrogen-bonded H₂O, whereas the (weak) feature at 3684 cm^{-1} is associated with the stretching mode of free OH-groups (*i.e.* non-hydrogen-bonded, dangling O—H bonds).^{151,152} The lower line shows the spectrum of 1.08 ML H₂O adsorbed on a surface pre-covered with hydrogen ($\theta_{\text{H}} = 1$). The feature at 3383 cm^{-1} is broader, more intense, and has become more asymmetric than for the bare surface. A small shoulder starts to appear at ~ 3500 cm^{-1} . The peak assigned to free OH-groups is not observed as clearly as on the bare surface. We note that when

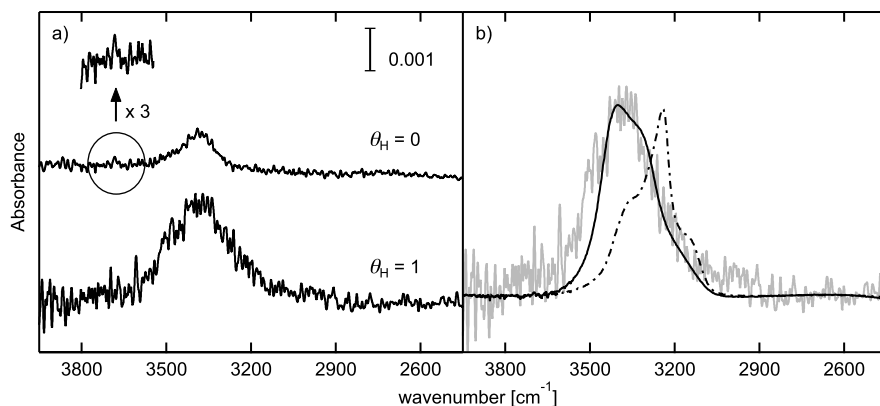


Figure 8.7 a) RAIRS spectra of ~ 1 ML H_2O adsorbed on Pt(533) where $\theta_{\text{H}} = 0$ (upper line) and $\theta_{\text{H}} = 1$ (lower line). b) Comparison of RAIRS spectrum where 1 ML H_2O is adsorbed on a fully hydrogen covered Pt(533) surface (grey line) to 45 ML ASW (solid black line) and 45 ML Cl (dash-dotted line) on Pt(533).¹⁵⁰ The spectra for 45 ML H_2O have been divided by 100.

H_2 and H_2O are co-adsorbed no feature around 1150 cm^{-1} is observed on Pt(533). This is in contrast to observations on Pt(111).^{88,89,92}

8.4 Discussion

In this section we will discuss both adsorption and reactivity of H_2O on the (partially) deuterium-covered Pt(533) surface. We will move from adsorption on to reactivity and finally argue that they are related. However, first we address deuterium adsorption without co-adsorbing water.

The procedure used to create partially deuterium-covered surfaces leaves in all of our experiments an amount of deuterium on the surface that is at least equal to the amount required to saturate the steps. This does not *a priori* mean that also all step sites are occupied when subsequently dosing water at ~ 100 K. Partitioning of deuterium between terrace and steps sites could take place, leaving part of the steps unoccupied. However, recent DFT calculations for an accurate potential energy surface (PES) for hydrogen dissociation on Pt(211) indicate that the binding energy of a hydrogen atom at step sites is ~ 0.35 eV larger than at any terrace site.⁶⁹ Olsen *et al.* find that adsorption of hydrogen at steps remains energetically more favorable than adsorption on all considered terrace sites up to saturation of the top edge of the (100) steps. At saturation of step sites, the H : Pt_{step} ratio is 1 : 1. Furthermore, an additional barrier of 0.1 eV compared to diffusion along the terrace is found for diffusion from a step site onto the terrace, especially in the downward

direction (“across the step”). Experiments probing diffusion on stepped platinum surfaces have also found that for the miscut required to create the (533) surface diffusion perpendicular to the surface is hampered relative to diffusion across the (111) terrace.⁷³ Preliminary experiments performed in our lab that probe exchange between hydrogen and deuterium separately adsorbed onto step and terrace sites indicate that exchange between steps and terraces is limited for partially and fully saturated surfaces. We therefore believe that in our experiments, pre-dosed deuterium saturates the (100) steps (almost) completely with any additional deuterium residing on (111) terraces when we start co-adsorbing H₂O.

We have discussed the desorption spectra from the bare platinum surface in chapter 3.3.3. Briefly, we ascribe the α_1 peak to desorption of water molecules that have been stabilized by the presence of (100) steps, the α_2 peak to desorption of water from terrace sites, and the α_3 peak to desorption from the water multilayer.

Pre-adsorption of deuterium drastically alters TPD spectra for this stepped surface. The observed stabilization of water on the bare Pt(533) surface is removed entirely when pre-adsorbing deuterium at the steps (figure 8.2b). The same observation was reported when steps were covered with CO prior to adsorbing water.²⁷ We have repeated those experiments with CO and find the same results (not shown here). In both cases, we observe that water desorption strongly resembles desorption from the bare Pt(111) plane at 171 K. The increase in the β_1 peak desorption temperature with increasing water coverage in the range $0 < \theta_{\text{H}_2\text{O}} < 1$ ML is also observed on both Pt(111) and D_{step}/Pt(533). A difference between our spectra and those taken for the (111) surface occurs in the leading edges of the desorption traces. For Pt(111) these coincide, whereas for D_{step}/Pt(533) they do not overlap. For Pt(111), the apparent zero-order desorption kinetics have been interpreted as a result of a coexistence of a condensed water phase with a 2-dimensional gas at equilibrium.²¹ Large patches of a condensed phase have been observed at lower surface temperatures by STM on broad (111) terraces.²⁸ The difference we observe in the leading edges suggests that, on Pt(533), the (100) steps inhibit coexistence of such a two-phase system at equilibrium. We note that the first layer of water on Pt(533) does wet the surface, though. The β_2 peak only appears when β_1 has saturated. It is also noteworthy that an equivalent of 1 ML H₂O interacts with the surface, since the integral of β_1 equals that of the sum of α_1 and α_2 . This is not surprising when noting that DFT calculations indicate that hydrogen atoms at steps sites adsorb on the outer edge of the step.⁶⁹ Therefore, saturating the (100) steps with deuterium does not block adsorption sites for water, but does alter the binding energy. For CO adsorption on steps, Grecea *et al.* conclude that CO sterically blocks water from the stronger binding sites. Our results imply that deuterium does not sterically block water adsorption, but causes destabilization through an electronic effect.

For the deuterium-saturated surface, additional destabilization is observed (figure 8.2a). Water desorbs from D_{max}/Pt(533) in a single peak that shows, well below

$\theta_{\text{H}_2\text{O}} = 1 \text{ ML}$, multilayer desorption characteristics. The desorption temperature of γ_1 equals that of multilayer desorption from Pt(111) and the observed overlapping leading edges imply zero-order desorption kinetics. We recently found the same behavior for water desorbing from deuterium-saturated Ni(111)¹⁵³ and implied that it was due to hydrophobicity of the surface. The same appears to be the case here. If the deuterium-covered Pt(533) surface is hydrophobic, water will form 3-dimensional structures at coverages well below $\theta_{\text{H}_2\text{O}} = 1 \text{ ML}$. When large enough, these 3-dimensional, multilayered structures will show zero-order desorption kinetics with a peak temperature equal to that of water desorbing from flat ASW multilayers.

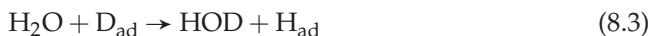
Our RAIRS spectra support this structural difference between 1 ML H_2O on bare and deuterium-covered Pt(533). Figure 8.7a clearly shows that upon pre-dosing hydrogen, the hydrogen-bonded OH stretch absorption near 3400 cm^{-1} broadens significantly. Increased disorder causes such broadening.¹⁵⁴ In figure 8.7b we compare the RAIRS spectrum of 1 ML H_2O adsorbed on the fully hydrogen covered Pt(533) surface to RAIRS spectra for bulk (45 ML) ASW and crystalline ice (CI) on Pt(533) published by Backus *et al.*¹⁵⁰ Our spectrum closely resembles the spectrum they obtained for 45 ML ASW. This shows that indeed ASW is formed at coverages of only 1 ML H_2O .

An additional observation supports our claim for 3-dimensional ASW water growth on the deuterium-covered surface. We noticed in figure 8.2a a slight, but consistent change in desorption rate at the leading edge of the γ_1 peak at $\theta_{\text{D}} > 0.7 \times \theta_{\text{max}}$, which leads to a double peak structure. Such a deflection in TPD spectra was previously observed when growing ASW layers on, amongst other substrates, Pt(111).^{24,25} The deflection has been shown to result from a phase change of ASW to CI during the temperature ramp. For 25 bilayers of ASW deposited on Pt(111) at 22 K, the crystallization occurs at $\sim 158 \text{ K}$.^{21,24} We observe the deflection in our TPD spectra for, what we claim are, multilayer 3-dimensional ASW clusters at exactly the same temperature. Therefore, not only do we believe that deuterium-covered Pt(533) is hydrophobic and results in growth of ASW “snowballs”, we observe the phase change in these “snowballs” to crystalline ice.

The shift in the β_1 peak desorption temperature for $\theta_{\text{step}} < \theta_{\text{D}} < \theta_{\text{max}}$ observed in figure 8.6 indicates a gradually decreasing binding energy for water with increasing concentration of deuterium on (111) terraces. Interestingly, Petrik and Kimmel observed a significant stabilization of water adsorbed on the Pt(111) surface with increasing deuterium coverages up to $\sim 0.25 \text{ ML}$.⁹⁰ Their TPD spectra show a distinct peak at $\sim 176 \text{ K}$ that appears at the (almost entire) expense of the 171 K peak. The (111) terraces on Pt(533) do not reproduce this behavior for $\theta_{\text{H}_2\text{O}} \sim 1 \text{ ML}$. Adsorption of deuterium on to approximately 1/4 of all terrace sites does not result in any significant change in water TPD spectra. Beyond this deuterium coverage, the peak temperature gradually shifts at a rate of approximately 18 K ML^{-1} pre-

adsorbed deuterium. For Ni(111), we have observed similar behavior but with a drop in peak desorption temperature of 25 K ML⁻¹.¹⁵⁵ On Ni(111), where hydrogen atoms cluster to form islands, it was speculated that it results from a decreasing (D₂O)_x cluster size above a certain deuterium coverage that leaves no space for ring-shaped water hexamers to adsorb on bare patches of the Ni(111) surface. For Pt(533), the same phenomenon explains our observations. The 4-atom wide terrace is large enough to support ring-shaped water hexamer structures in contact with bare platinum. DFT calculations indicate that hydrogen atoms primarily adsorb at and near step sites on platinum.⁶⁹ However, when those sites are occupied, additional deuterium must adsorb onto terrace sites further removed from the step, thereby reducing the remaining size of bare (111) patches. If deuterium interferes with formation of hexamer rings from post-dosed water, increasing concentrations of deuterium may result in formation of shorter or more branched water chains. Such structures have fewer hydrogen bonds per water molecule with decreasing cluster or chain size and are therefore stabilized less by the hydrogen-bond network. Apparently, this process is gradual and results in the gradual decrease in peak desorption temperature as observed in our TPD spectra. Although this argument, based on a steric effect between D_{ad} and H₂O, may explain our observations, we do not exclude that also an electronic effect could lie at the origin of our observations. Amongst others, STM imaging and DFT calculations may provide better understanding.

Our TPD spectra of both $m/e = 3$ and 4 and $m/e = 19$ and 20 indicate that the Pt(533) surface induces thermo-neutral exchange between H from H₂O and D_{ad}.



Such exchange has also been observed and studied on Pt(111)⁸⁹ and Pt(100)⁹¹ surfaces. For Pt(533), figures 8.4 and 8.5 show that this exchange reaction is dependent on the amounts of water and deuterium present. We observe that the exchange peaks when deuterium atoms saturate the (100) steps and cover half of the (111) terraces. The kinetics therefore seem dependent on a $\theta_{\text{D,terr}} \times (1 - \theta_{\text{D,terr}})$ term. This suggests that the rate of reaction improves when at least some of the post-dosed H₂O interacts directly with bare platinum atoms in the (111) terrace. However, formation of HD and HOD is not shut down when the surface is fully covered with D_{ad} and we can conclude that reaction occurs both in a mixed deuterium/water phase in contact with the metal and in a system where water is adsorbed as a multilayered structure on top of the hydrophobic deuterium-covered surface, though exchange would be faster in the former one.

For the latter case, it is instructive to consider the exact dependencies observed. For the deuterium-saturated surface we observe that HOD formation is linear up to 2 ML of water desorbing from the surface (inset in figure 8.5b). For the step-saturated surface, we observe curvature in the HOD formation already at $\theta_{\text{H}_2\text{O}} = 1.2$ ML (inset figure 8.5a). This strongly suggests that in the latter case, the

total amount of D on the surface has been depleted significantly. The same figures also illustrate that multilayers of water simply act as a buffer for deuterium atoms originating at the surface. Once deuterium atoms have been exchanged at the metal surface, they quickly move into the multilayer regime through exchange:



This exchange has been studied for thicker ASW layers and was found to be very rapid.¹⁵⁶ Also for Pt(100) exchange as in equation (8.4) was shown to be rapid in comparison to exchange as in equation (8.3).⁹¹ The quick exchange of D between water molecules causes the isotopic fraction of HOD in multilayers to reach a constant value with increasing water coverage when enough deuterium is present at the start, *i.e.* at $\theta_{\text{D}} = \theta_{\text{max}}$. For significantly lower starting surface concentrations (*e.g.* $\theta_{\text{D}} \approx \theta_{\text{step}}$), D_{ad} is depleted to an extent that, with increasing water coverage, the HOD and D_2O partitioning drops at higher H_2O doses.

Finally, we turn to the observed differences in the ratio for step and terrace desorption for HD and D_2 . Figure 8.4b shows that post-adsorption of 1 ML H_2O only yields HD desorption from steps when the initial deuterium coverage on terraces is (close to) zero. Logically, if deuterium is only present at steps, exchange can only occur there. This observation actually also strengthens our belief that atomically bound hydrogen (deuterium) at steps does not significantly diffuse to terraces in any of our experiments. As noticed before, when increasing the terrace deuterium coverage, both HD and HOD production go up and clearly peak for terrace desorption when terraces are approximately half filled with D_{ad} . Exchange at steps sites is not affected much by the terrace deuterium concentration, as can be concluded from the absence of a significant change in HD desorption from steps. On the other hand, D_2 desorption from terraces is found to increase rapidly with increasing deuterium pre-coverage. Desorption of D_2 from steps is significantly less affected when increasing deuterium pre-coverage. These observations seem contradictory, since with more deuterium present on terraces, exchange at the terraces would be expected to become more dominant. Figure 8.5b quantifies this behavior for increasing H_2O post-dose with $\theta_{\text{D}} = \theta_{\text{max}}$. Isotopic exchange occurs consistently almost twice as much on steps as compared to terraces.

The key to understanding this apparent contradiction lies in the connection between structure and reactivity. As we argued earlier, increasing the deuterium surface concentration on terraces induces hydrophobicity of the surface and 3-dimensional ASW growth. We believe that these “snowballs” are preferentially located at steps, because, if they do, this would explain the bias of the exchange reaction at steps. With increasing D_{ad} pre-coverage on terraces, reactivity initially increases as long as D_{ad} and H_2O can co-exist on terraces and both are in contact with the metal surface. However, when the terrace deuterium coverage is high enough, H_2O molecules are repelled toward steps, initiating 3-dimensional ASW

growth. For the terraces, this lowers HD formation and increases D₂ formation. Since exchange now primarily occurs at and near steps, the total exchange drops.

From our results we can not conclude via which mechanism, or intermediate species, hydrogen exchange takes place. Literature suggests the formation of an hydronium-type species.^{89,93} Based on our results, we can neither confirm nor disprove this claim. More detailed spectroscopic studies and DFT calculations may provide more insight in this matter.

8.5 Conclusion

We have observed various effects on the interaction of Pt(533) with water when deuterium is pre-adsorbed. First, the preference of deuterium to adsorb at step edges nulls the stabilization of water at steps through an electronic effect. Deuterium atoms at step edges do not block adsorption sites for water and water still wets the entire (111) terrace. However, co-existence of water as both a condensed phase and a 2-dimensional gas phase does not occur as it does on larger (111) terraces. Formation of smaller, less ordered water structures seems to replace formation of hexamer ring structures with increasing deuterium coverage. Near deuterium saturation, water preferentially forms 3-dimensional ASW clusters at the steps. These ASW clusters are large enough at an equivalent amount of less than 1 ML to allow for observation of its phase transition to crystalline ice. Although exchange of D_{ad} with H₂O occurs both at steps and terraces and is dependent on both surface coverages, the preference of water molecules to cluster at the step sites on the hydrophobic, deuterium-saturated Pt(533) surface biases exchange toward steps.